Internal representation of hippocampal neuronal population spans a time-distance continuum

Caroline Haimerl[a,1], David Angulo-Garcia[b,1], Vincent Villette[c], Susanne Reichinnek[c], Alessandro Torcini[d,e,f], Rosa Cossart[c,2], and Arnaud Malvache[c,2]

[a]Center for Neural Science, New York University, New York, NY 10003; [b]Grupo de Modelado Computacional–Dinámica y Complejidad de Sistemas, Instituto de Matemáticas Aplicadas, Universidad de Cratagena, 130001, Cartagena, Colombia; [c]Aix Marseille University, INSERM, Institut de Neurobiologie de la Méditerranée (INMED), Turing Center for Living Systems, 13007 Marseille, France; [d]Laboratoire de Physique Théorique et Modélisation, Université de Cergy-Pontoise, CNRS, UMR 8089, 95302 Cergy-Pontoise, France; [e]Aix Marseille Univ, INSERM, Institut de Neurosciences des Systèmes (INS), 13007 Marseille, France; and [f]CNR–Consiglio Nazionale delle Ricerche–Istituto dei Sistemi Complessi, 50019 Sesto Fiorentino, Italy

Edited by Charles F. Stevens, The Salk Institute for Biological Studies, La Jolla, CA, and approved January 31, 2019 (received for review October 24, 2017)

The hippocampus plays a critical role in episodic memory: the sequential representation of visited places and experienced events. This function is mirrored by hippocampal activity that self organizes into sequences of neuronal activation that integrate spatiotemporal information. What are the underlying mechanisms of such integration is still unknown. Single cell activity was recently shown to combine time and distance information; however, it remains unknown whether a degree of tuning between space and time can be defined at the network level. Here, combining daily calcium imaging of CA1 sequence dynamics in running head-fixed mice and network modeling, we show that CA1 network activity tends to represent a specific combination of space and time at any given moment, and that the degree of tuning can shift within a continuum from 1 day to the next. Our computational model shows that this shift in tuning can happen under the control of the external drive power. We propose that extrinsic global inputs shape the nature of spatiotemporal integration in the hippocampus at the population level depending on the task at hand, a hypothesis which may guide future experimental studies.

hippocampus | space representation | time representation | neural model | attractor network

Episodic memory holds information about spatial (where), nonspatial (what), and temporal (when) components of life experiences (1). While spatial and nonspatial information is available in the environment (e.g., proximity to a wall, presence of a given object), temporal information is an abstract concept anchored in the dynamics of the brain. In rodents, both distance and duration have been found to be represented in the hippocampal formation, a brain area critically involved in episodic memory. This has been reported in CA1 (1–5), CA3 (6, 7), and the medial entorhinal cortex (8, 9). Specifically, it has been shown that when rodents run in place on a wheel or a treadmill (in the absence of movement in the laboratory reference frame), hippocampal neurons fire in a sequence whose dynamics can be driven by elapsed time (2) or traveled distance (4).

While information about distance is provided primarily by speed and self-motion cues, the sequential firing of neurons in this paradigm is most likely self-organized locally at the circuit level, as it occurs without any ordered arrangement of external inputs. Such internal sequences representing information relative to the past (e.g., elapsed time, traveled distance) must be generated by an integration in time (in the mathematical sense) of spatiotemporal information. Thus, it might not be coincidental that duration and distance internal representations have been observed in the same networks (4). While mathematical models have been able to reproduce the integration of time and space in different experimental paradigms (10), whether the same network structure can switch from encoding distance to duration remains unknown.

A particularly relevant model of network structure in this background are continuous attractor neural networks (CANNs) (11, 12), which have been found to generate sequences of neuronal activation from nonsequential external inputs (13–15). In such networks, neighboring neurons within a sequence are synaptically linked, forming a circular network (or ring attractor network). They also require the presence of global feedback inhibition that allows for the firing of a few neighboring neurons at a given time (i.e., an activity bump) (16). This type of network structure accurately describes the structure of the pyramidal layer in which excitatory neurons display recurrent connections (17, 18), which in principle can lead to a circular network, and interneurons provide strong feedback inhibition (19). The main input driving the sequence generation in such network models is a theta oscillation, that is, a 6- to 10-Hz signal present in local field potential recordings in the hippocampus when rodents are running (20). Wang et ;al. (13) showed that a reduction in the power of the theta oscillation induced by silencing the medial septum led to the interruption of internal sequence generation. Therefore, CANNs appear to be a good candidate model for evaluating whether the same network organization can ground sequences encoding elapsed time and/or distance.

Here, combining data analysis of long-term sequence dynamics across days and network modeling, we asked whether the same circuit can combine and/or alternate between traveled distance and elapsed time (duration) representations, and we describe a candidate mechanism by which such switching could occur. Toward this

Significance

The hippocampus organizes experience in sequences of events that form episodic memory. How are time and space internally computed in the hippocampus in the absence of sequential external inputs? Here we show that time and space are integrated together within the hippocampal network with different degrees of tuning across days. This was found by recording the activity of hundreds of pyramidal cells for several days. We also propose a mechanism supporting such spatiotemporal integration based on a ring attractor network model: the degree of tuning between space and time can be adjusted by modulating the power of a nonsequential external excitatory drive. In this way, the hippocampus is able to generate a spatiotemporal representation tuned to the task at hand.

Author contributions: C.H., D.A.-G., A.T., R.C., and A.M. designed research; C.H., D.A.-G., V.V., and S.R. performed research; C.H., D.A.-G., and A.M. analyzed data; and C.H., D.A.-G., and A.M. wrote the paper.

The authors declare no conflict of interest.

This article is a PNAS Direct Submission.

Data deposition: All data and codes used in analysis and for the model are available on GitHub https://github.com/CarolineHaimerl27/duration_distance_coding.git.

[1]C.H. and D.A.-G. contributed equally to this work.

[2]To whom correspondence may be addressed. Email: rosa.cossart@inserm.fr or arnaud.malvache@inserm.fr.

This article contains supporting information online at www.pnas.org/lookup/suppl/doi:10.1073/pnas.1718518116/-/DCSupplemental.

aim, we quantified the components of duration and distance dimensions in sequences of neuronal activation occurring in mice spontaneously running on a self-paced treadmill. Neuronal activity was sampled in CA1 using two-photon calcium imaging as described previously (5). We found that the same network could alternate between states, sometimes combining information about duration and distance. As suggested by Salz et al. (6), who reported equivalent duration- and distance-related activities among CA1 and CA3 cells, we made the assumption that CA1 activity reflects activity in CA3 in the absence of movement in the laboratory reference frame, and thus modeled a recurrent network with feedback inhibition (CANN) driven by theta oscillation. The speed of the mouse was fed into the network through the modulation of theta oscillation power. We found that such network exhibits dynamics suitable for a dual representation of both duration and distance. Finally, by fitting experimental data, we demonstrate that the same circuit can switch between representations under the influence of a global external signal.

Results

We recently showed that in the absence of external constraints (no task, no reward), CA1 activity self-organizes into sequences of neuronal activation ("run sequences") representing distance or duration during spontaneous run episodes in head-fixed mice running on a nonmotorized, uncued treadmill (5). After expanding this dataset with additional calcium imaging experiments, we further analyzed the spatiotemporal representation in run sequences from 34 imaging sessions ($n = 7$ mice). In these experiments, mice were head-fixed under the objective of a microscope. Expression of calcium indicator GCaMP5, 6m, or 6f was virally induced, and surgery was performed to provide a chronic optical access to the pyramidal cell layer of dorsal CA1 (5, 21). During the 20- to 30-min imaging sessions, 140 ± 47 neurons were identified as being active within the $400 \times 400\ \mu m^2$ field of view; 39 ± 11% of them were activated in run sequences (Fig. 1 *A* and *B*; 28 ± 14 run sequences per imaging session).

We first applied our previously described method (5) for quantifying distance/duration representation by looking at correlations between running speed and sequence slopes in the spatiotemporal domain, respectively. The network was considered to represent distance if there was a significant correlation between temporal slopes and running speeds (i.e., spatial test), while it was classified as representing duration if spatial slopes and running speeds were significantly correlated (i.e., temporal test); a network could be classified as representing both time and distance, as partial correlations could be found in both tests (5). The strength of distance/duration representation was defined as the value of the Spearman rank correlation. Imaging sessions were scattered in this 2D space (Fig. 1*C*), with sessions with both representations were significantly present. These results suggest that distance-only and duration-only representations are the two extreme cases of a more global, mixed spatiotemporal representation (a continuum).

We next derived a method that tests for the presence of a combination of duration and distance representations in the dynamics of run sequences (*Materials and Methods* and *SI Appendix*, Fig. S1). The basic principle is to combine the spatial and the temporal slope into a single value and test the dependence of this value with an adequate parameter that depends on speed (i.e., spatiotemporal test). Our test has the advantage of being less sensitive to measurement noise inherent to large-scale and fast calcium imaging. Thus, it can detect spatiotemporal representation where the two independent tests for distance and duration representation cannot (*SI Appendix*, Fig. S1*D*).

From the results of the temporal, spatiotemporal, and spatial tests, we could define five categories of representations (Fig. 1*D* and *SI Appendix*, Fig. S1) ranging from "duration-only" (case 1) to mixed forms (cases 2–4) to "distance-only" (case 5). We found

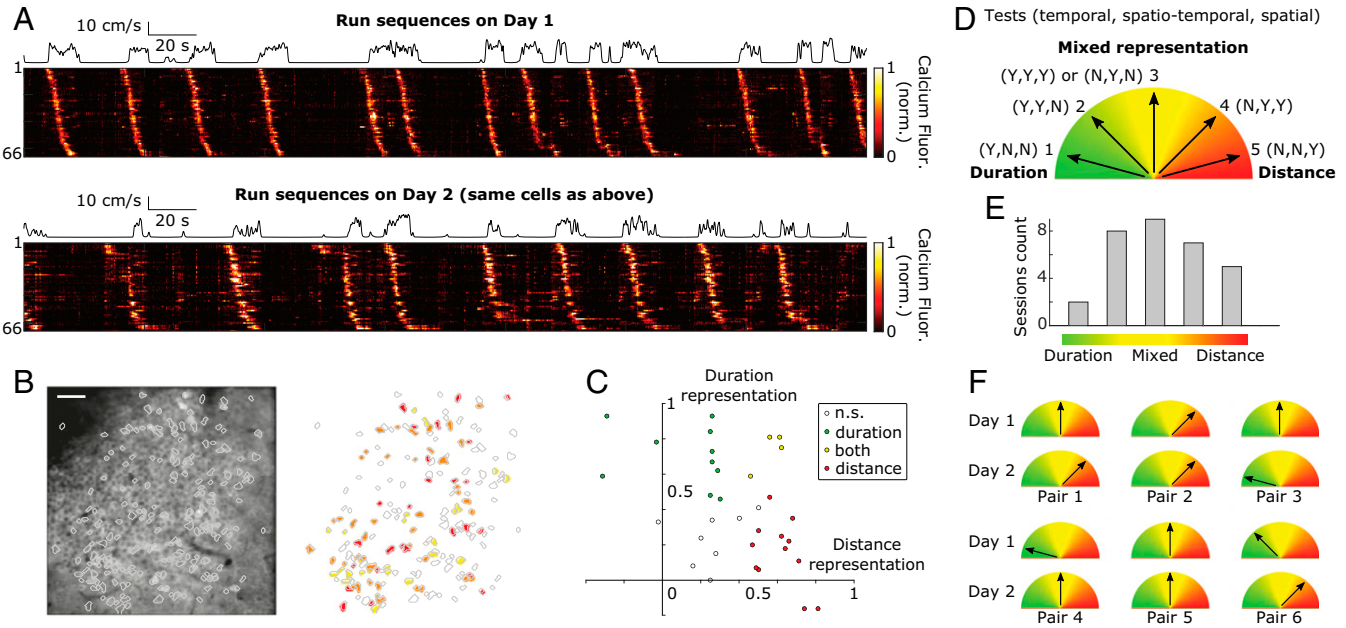

Fig. 1. Mixed distance and duration representation in CA1. (*A*) Calcium fluorescence (heatmap) of CA1 neurons participating to run sequences in consecutive imaging sessions. Cells have been selected and ordered with respect to their activity in the first imaging session (*Top*). The black line represents speed of the mouse. (*B*) Example field of view in the CA1 pyramidal cell layer and contours of active cells across two consecutive sessions (*Left*) and color-coded map of cell participating in run sequences (*Right*). Red and yellow represent participation on the first or second day only (respectively); orange represents participation on both days. (Scale bar: 50 μm.) (*C*) Spatiotemporal representation of the 34 imaging sessions in the distance/duration 2D space. The *x*-axis (*y*-axis) represents Spearman correlation values between temporal (spatial) sequence slopes and running speed. (*D*) Rule and drawing defining the five categories of spatiotemporal representation from the results of the temporal, spatiotemporal, and spatial tests, Y/N (yes/no) indicate significance ($P < 0.05$). (*E*) Distribution of the 34 imaging sessions across the spatiotemporal representation. (*F*) Schematic of the change in spatiotemporal representation on two consecutive days for six imaging session pairs.

that the imaging sessions that displayed a significant representation (31 of 34 sessions) were distributed across these five categories (Fig. 1*E*), confirming the capability of CA1 neurons to combine information about duration and distance (4).

We next analyzed the evolution of this representation in time, using repeated imaging sessions from the same network for two consecutive days. In six pairs of imaging sessions ($n = 3$ mice), we found that $60 \pm 12\%$ of the cells participating in run sequences on the first day were recruited again in run sequences on the next day (Fig. 1 *A* and *B*), and that the ordered activation of these sequence-stable cells was significantly preserved ($8 \pm 1\%$ change in relative order; 99.9999th percentile after reshuffling). Focusing on sequence-stable cells only, we again computed the different tests for spatiotemporal representations; in four of six paired sessions, the same set of neurons exhibited a change in dynamics with respect to speed (Fig. 1*F*), indicating that the same network could adjust its relative representation of duration and distance.

We next designed a numerical model of the neural network to study which properties are required to enable a change in spatiotemporal integration. As discussed in the introduction, we chose a CANN. To best model a CANN grounding both duration and distance representations, we searched for specific network properties in our experimental data. As shown by Villette et al. (5), run sequences could restart where they stopped after an immobility period if the pause was shorter than 2 s. In addition, run sequences could repeat one after another within continuous long run episodes. The former property suggests that there is some kind of short-term memory within the network that holds information about the last active neuron. The latter indicates the existence of functional links between first and last neurons in run sequences and supports the hypothesis of periodic boundaries in the CANN.

We designed a recurrent neural network with global feedback inhibition (CANN; *Materials and Methods* and Fig. 2*A*) that when excited by a global external input, allows for the formation of a localized subgroup of firing neurons (activity bump) (11, 12). The connectivity matrix of the network integrates both local excitatory connections and a global feedback inhibition (*Materials and Methods* and Fig. 2*B*). The local excitatory connections were spatially asymmetric (11), biasing the propagation of the activity bump toward one direction (*Materials and Methods* and Fig. 2*B*), as observed in experimental data in which run sequences are always played in the same order. We simulated the neural activity of the network using the following firing rate model (22):

$$\tau \frac{dm(i,t)}{dt} = -m(i,t) + f(I_R(i,t) + I_E(t)),$$

where $m(i,t)$ is the firing rate of neuron i at time t, τ is the relaxation time constant ($\tau = 10$ ms), f is a threshold linear function, I_R is the recurrent inputs from local excitation and global inhibition, and I_E is the global external input. To account for the experimental observation that the same neurons are always recruited at the start of the run sequence, we added a bias on neuron excitability with respect to their position in the ring network (*Materials and Methods*). A time-constant external input to all cells, $I_E(t) = I_0$, leads to a repetitive (circular) sequential activation of cells (Fig. 2*C*, *Top*) that mimics experimental data. In this simplified framework, the asymmetry in the connections determines the speed of activity flow, which thus is independent of the amplitude of the constant external input to the system.

Following a demonstration that theta oscillations are required to generate internal sequences, the model proposed by Wang et al. (13) used a similar CANN driven by an oscillatory input mimicking theta oscillation. It modulates the network activity so that at each rising phase, the most excitable cells become active. This activity bump propagates until the input power sets below threshold; at the trough, all cells are silent (Fig. 2*C*, *Bottom*). The group of cells active during a cycle shifts from cycle to cycle, producing an overall sequence. To allow the network to keep track of past activity from one cycle to the next, Wang et al.'s (13) model included synaptic facilitation and depression, which, along with changes in intrinsic excitability (23), are well-known mechanisms for short-term memory in the hippocampus (24–26). Facilitation hereby mimics the effect of residual calcium levels at presynaptic terminals that increase with firing and boost excitability, thereby creating a memory effect. Depression represents the available resources of calcium, which decreases with the amount of firing and reduces excitability. Thus, we included theta oscillation $I_E(t) = I_\theta \sin(2\pi f_\theta t)$ and synaptic facilitation and depression in our model (*Materials and Methods* and *SI Appendix*, Fig. S2). Their time constants were heuristically chosen to be 300 ms (*SI Appendix*, Fig. S3). With such values, neurons reduce their firing within theta cycle bursts, and active neurons remain more excitable from one cycle to the next.

In this more comprehensive model (short-term plasticity and theta input), the cycle-to-cycle velocity of bump propagation is no longer constant over different input powers but instead exhibits a nonlinear relationship and displays a minimum velocity (Fig. 2*D*). This nonlinear relationship appears to increase both theta-modulated input and time-constant input (*SI Appendix*, Fig. S4). This is a counterintuitive result in which within a given amplitude range, increasing the amplitude of the input decreases the propagation velocity of the activity bump. Synaptic plasticities modulate the connectivity of the network and act on the propagation of the activity bump; the effective asymmetry (defined as the shift between the center of the activity bump and the center of the source term, $I_R + I_E$; *Materials and Methods*) has a similar nonlinear relationship with theta input power (Fig. 2*E*). Thus, the presence of short-term synaptic plasticity makes the network dynamics sensitive to external input power. This nonlinear feature is therefore a possible mechanism for the different sequence slope vs. speed relationships observed in experimental data that lead to the different spatiotemporal representations

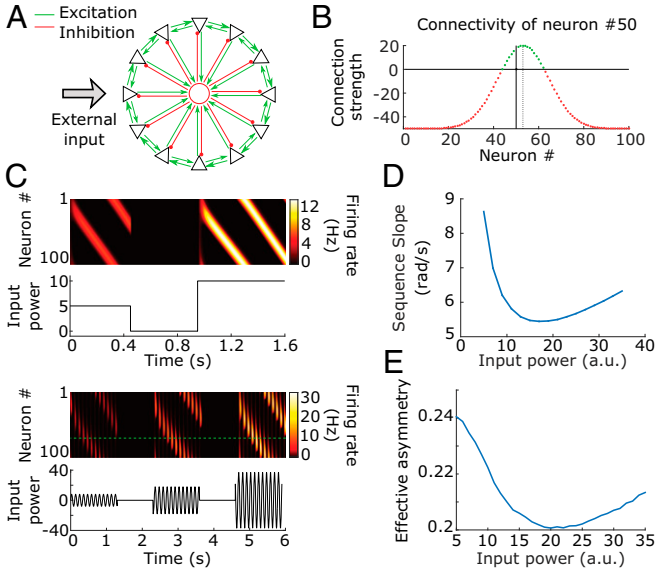

Fig. 2. Nonlinear neural sequence dynamics in CANNs. (*A*) Schematic of the CANN, a ring excitatory network with global feedback inhibition. (*B*) Total (excitatory + inhibitory) connectivity strength of neuron 50; note the asymmetry of the profile. (*C*) Simulated neuronal sequences triggered by transient constant input (*Top*) and theta input (*Bottom*). (*D*) Propagation velocity of the bump (or sequence slope) with respect to input power for the model with short-term plasticity and oscillatory input. (*E*) Effective asymmetry of the network connectivity with respect to input power in the model with short-term plasticity and oscillatory input.

(Fig. 1 *B–D*), provided that mouse speed is encoded in the amplitude of the global input and the range of amplitudes remains within a narrow window in which the dependence can be assumed as linear.

To test this latter hypothesis, we designed a speed-dependent input. Theta amplitude has been shown to increase with the running speed of an animal (26); thus, we assumed a linear relationship between theta amplitude and the speed of the mouse,

$$I_\theta(t) = I_0 + \beta(v(t) - v_0),$$

where I_0 is the mean theta power, β is the gain applied to speed, and v_0 is the median speed. The oscillatory input to the network carries speed information that will then be integrated by the CANN (Fig. 3*A*). Therefore, the nonlinear relationship between slope velocity and input amplitude provides a candidate mechanism for integrating time or distance in a continuous fashion through a change in input average strength.

We next show that this qualitative behavior can be used to quantitatively reproduce experimental data. First, we heuristically identified the span of the 2D parameter space consisting of theta power, I_0, and asymmetry in connectivity, δ, where values of experimental slopes could be obtained. From this phase diagram (Fig. 3*B*), we see that the asymmetry parameter δ sets the average value over which the slopes change, while the theta power parameter I_0 explores the different spatiotemporal representations.

We then performed a data fitting procedure to assess the ability of the proposed model to describe real data. Indeed, the diversity of mouse behavior and the range of run sequence slopes across experiments required that the neural network be robust to changes in time scale. Furthermore, as shown previously, neural sequences are not very stable from one day to the next in terms of cell participation, but the cell order is mostly preserved (27). This indicates that functional links between consecutive cells in the sequence are preserved across days. Thus, the goal was to obtain quantitative fits of the slope vs. speed behavior across all data without any arbitrary adjustment of the network's parameters. To do so, for each session, we extracted the triplet of values (δ, I_0, β) that minimized the sum of squared errors between the model slopes (Fig. 3*B*) and the slopes of all recorded sequences during the session, as a function of the animal's speed (*Materials and Methods*). To quantify the goodness of the fit, we used the root mean of normalized squared error (RMNSE), which quantifies the mean relative deviation between data and model fit (*Materials and Methods*). Across 34 sessions, the fitting procedure reproduced the experimental data within an error <20% (median RMNSE = 0.19), which is a fairly good approximation considering the purely deterministic nature of the model compared with the highly noisy data. Two example fits for a distance and duration representation are shown in Fig. 3*C*.

We then analyzed the relationship between β and median speed, v_0, in a given session. An expected anticorrelation could be observed (Pearson $\rho = -0.55$; $P < 0.01$) (Fig. 3*D*). This reveals

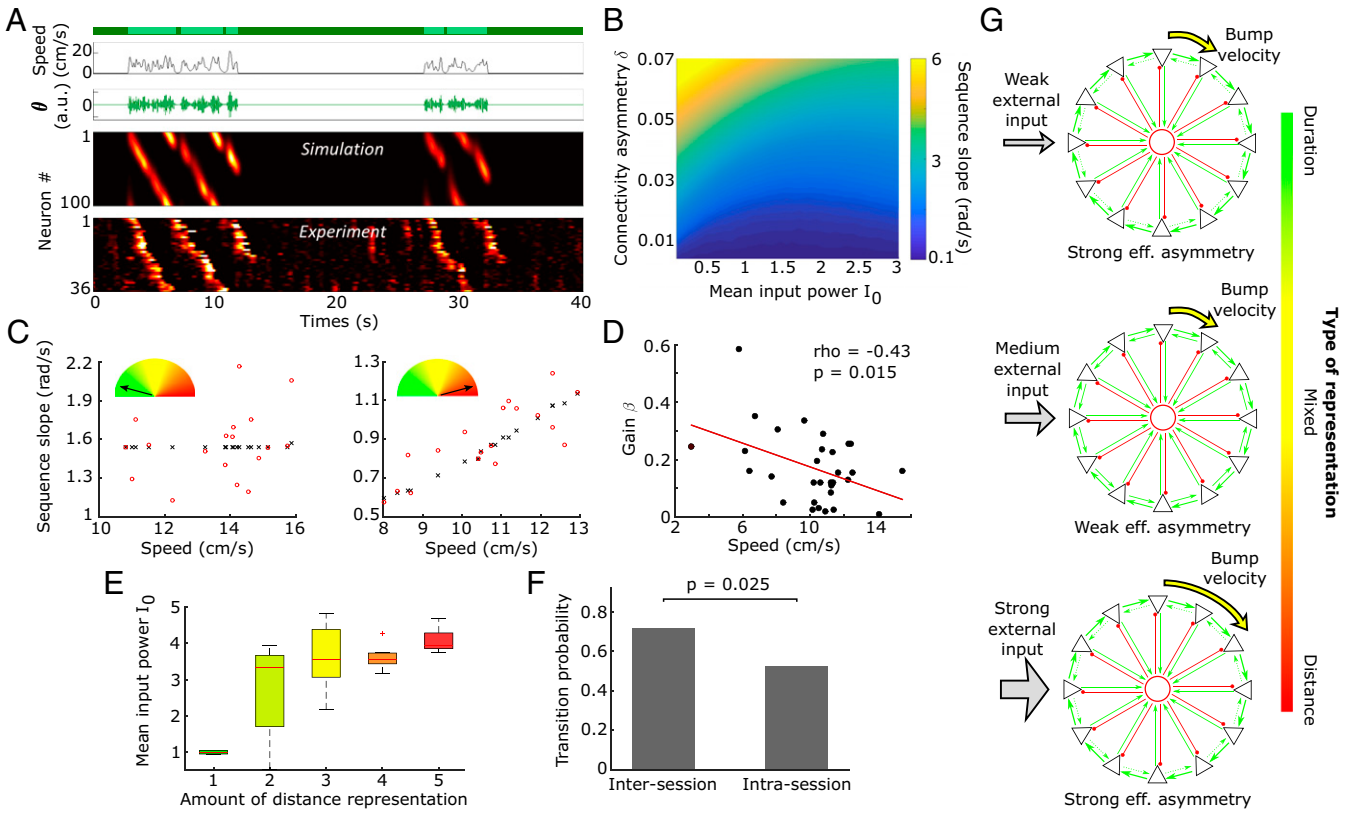

Fig. 3. Spatiotemporal representation in CANNs. (*A*) Realistic sequence generation; actual speed of the mouse (*Top*; dark green, immobility period; light green, run episode), artificial theta oscillation modulated in amplitude (*Top Middle*), sequences of neuronal activation generated by the CANN (*Bottom Middle*) and actual neuronal activity recorded in CA1 (*Bottom*). (*B*) Phase diagram in the (I_0, δ) space with color-coded slope velocities in rad/s. (*C*) Sequence slope vs. speed for duration (*Left*) and distance (*Right*) representation, experimental (red dots) and fitted (black crosses and lines) data. (*D*) Scatterplot of the fitted gain parameter β and the corresponding median speed of the mouse for the 34 sessions. Linear regression shows a linear dependence between these two quantities (Pearson). (*E*) Distribution of the mean theta power, I_0, according to the distance representation, showing a clear correlation (Spearman's $\rho = 0.73$; $P = 5e\text{-}6$). (*F*) Probability for a transition in coding across sessions (inter) and within sessions (intra). A higher probability for a shift in coding is expected on a longer time scale (χ^2 test, $P < 0.05$). (*G*) Schematics of the spatiotemporal representation mechanism. For three different input powers, the network effective asymmetry and sequence dynamics (bump velocity) change nonlinearly.

the homeostatic role of the modulatory parameter β, which upon acting on the mouse's speed, avoids the uncontrolled increase of the input to the CANN and allows for existence of the different spatiotemporal representations in a reduced parameter space.

We finally studied whether such parameters revealed any particular feature with respect to the spatiotemporal representation as defined in Fig. 1*C*. I_0 showed a correlation with the extent to which distance was represented (Spearman test, $P < 1e\text{-}5$) (Fig. 3*E*). This result was also expected, since "duration-only" sequences (case 1) occur when theta power is distributed around the minimum of the U-shaped function in Fig. 2*D* (at small inputs), while "distance-only" (case 5) are expected to occur in the right part of the U-shaped function (large inputs). Taking advantage of this correlation, we quantified how the distributions of I_θ changed from one recording session to the next (intersession) and compared with the changes from one-half of a recording session to the other (intrasession). Fig. 3*F* shows that the distribution of I_θ shows larger intersession changes than intrasession changes (81% intersession vs. 52% intrasession; χ^2 test, $P < 0.05$). These results suggest that the space-time representation is more likely to change over longer time scales (*SI Appendix*).

To conclude, we have shown that a CANN with short-term synaptic plasticity has an effective asymmetry in its connectivity that nonlinearly depends on the input power (Fig. 2*E*). It is first anticorrelated with input power for low powers and then correlated with input power for high powers. This leads to a nonlinear dependence of the neural sequence dynamics with input power (Fig. 3*G*). These observations demonstrate that a network integrating speed information can be externally tuned to represent any combination of space and time, and that the changes in such representation are likely to occur over long time scales.

Discussion

The hippocampus is able to represent the diverse spatiotemporal components of experience, based mainly on either environmental inputs or self-generated and internally computed information. Based on empirical data, we show that two internally computed information components—duration and distance—are embedded in the sequences of neuronal activation that occur in CA1 when a mouse is running in place on a treadmill. Instead of recruiting two distinct networks of cells that would separately integrate the temporal or spatial dimensions, we demonstrate experimentally and theoretically that the same functional circuit organization can ground both representations. This conclusion was largely enabled by our experimental paradigm that provides a sufficiently wide temporal window on hippocampal dynamics and mouse spontaneous running behavior to cover a sufficiently large spectrum of spatiotemporal representations.

Those representations can be generated by a CANN that mimics a CA3 recurrent network. A theta oscillation modulated in amplitude by speed was used as an external input in our model, so that the network could integrate speed through the propagation of an activity bump. Theta oscillations carrying speed information have been reported experimentally (26); they are generated in the medial septum and directly modulate the activity of CA1 cells (28). It also has been shown that when neural activity in the medial septum is pharmacologically impaired, both theta oscillations and internal sequence generation in the hippocampus are affected (13). This result was supported by a model of sequence generation that was the basis of our modeling work.

We extended this existing framework to our experimental results by adding dependence between mouse speed and the amplitude of theta oscillation. We found that depending on the range of theta amplitude, the propagation velocity of the activity bump was either constant or linearly dependent on the speed of the mouse. Data fitting showed that these qualitative properties could be used to quantitatively reproduce experimental data. This result is explained by the presence of short-term synaptic plasticity, which dynamically influences the connectivity of the neural network. In the CANN considered here, this dynamic effect led to a nonlinear dependence of the bump propagation velocity on external input power. Importantly, facilitation turned out to be essential in the model for this nonlinear dependence; a model without dynamic facilitation only allows increases in velocity with increased external input. Short-term synaptic plasticity might not be the sole cellular mechanism by which bump propagation velocity varies nonlinearly with input. Indeed, short-term plasticity can also be supported by the plasticity of intrinsic excitability, such as postinhibitory rebound or spike adaptation (29). As synaptic plasticity, this intrinsic plasticity is frequently reported, is bidirectional, and occurs at various time scales (23).

Even though we only considered a linear dependence between mouse speed and theta amplitude, our results can be extended to a wide set of nonlinear functions as long as a rank correlation between I_0 and the animal's speed, v, is maintained. This can be easily verified by the fact that mean theta power is the key correlate with the type of representation. Therefore, any function that maps the speed into I_0 in a monotonic fashion can span the whole range of mean theta power in which time-distance representation information lies.

Quantitative analysis of the data fitting showed that the type of representation (e.g., duration vs. distance) is set by adjusting the mean power of the global excitatory drive to the network. The possibility that modulation of an external oscillatory input can change the mode of information processing in CA1 has been previously reported experimentally for gamma oscillations. Indeed, during slow gamma oscillations, CA1 activity is modulated by CA3 inputs and involved in memory processes, whereas during fast gamma oscillations, CA1 is rather functionally connected to the medial entorhinal cortex, a region that transmits current spatial information (30). Our study identifies a change in mean theta power as a possible way of shifting between spatiotemporal representations, but any global increase in excitability of the network would lead to the same effect (*SI Appendix*, Fig. S5). Thus, a neuromodulatory influence that changes the excitability of CA1 (31) could be another mechanism that sets the degree of distance and duration representations. Increases in theta power or in excitability should manifest as increases in the neuronal firing rate. Future experiments combining calcium imaging with electrophysiological measurements at the single neuron level could test whether a change in representation would be bound to a change in the firing rate, following our predictions.

We also observed that the gain of the linear relationship between speed and oscillation power was inversely proportional to the median speed. This suggests a form of homeostasis that normalizes the input, a process that is expected in the hippocampal network (32) and that could be explained by the presence of feed-forward inhibition (19). An important aspect of the fitting procedure is that it allowed us to assess the potential representation shift ability within a session, an analysis that was not possible to perform with the space-time test with experimental data due to downsampling.

Individual CA1 principal cells have been previously shown to represent both distance or duration, with different degrees of tuning at single-cell level within a given recording session (4). Here we took a different perspective by looking at the mean population dynamics (run sequence slope) of a recording session. We showed that in a given imaging session, sequential neuronal activations followed a rule for integrating space and time, and that this rule could change across imaging sessions. Across all our data, the rule spanned the whole time-distance continuum, from pure time to mix to pure spatial representations. This can be explained by a model of internally generated sequences that is able to shift its coding scheme while preserving its network organization (i.e., the identity and order of cell activation in the sequence).

Another relevant model of time, distance, and space has been proposed by Howard et al. (10), in which a hidden layer of leaky

integrate-and-fire neurons with different decay time constants maintains a trace of a stimulus. This first layer connects a second layer of neurons with adequate synaptic strengths to retrieve past events by performing a Laplace-like transform. This model nicely reproduces goal-motivated behavior, but predicts scale-invariant representations (i.e., the longer the memory, the less accurate the representation).

In our experimental paradigm, there were no discrete stimuli; mice were running spontaneously on an empty treadmill, and we did not observe the widening of firing fields at the end of the sequence (*SI Appendix*, Fig. S6), the signature of scale invariance. In the previous model, a modulation of inputs proportional to speed was used to implement path integration, but this modulation was removed for simulating time representation. With our model, any type of spatiotemporal representation can be generated without the need to remove the speed-modulated input. Further work is needed to combine our model of spatiotemporal representations for spontaneous behavior with the previous model for constrained behavior.

In a more general framework, CANN models for internal sequence generation can reproduce one-dimensional representations but lacks a second dimension when it comes to place cells in an open environment. It may be possible to extend this model to 2D using a toroidal manifold (22). It is also possible that place cell formation occurs through a different pathway that computes allocentric information (33) independent of distance and duration integration that we assume occur in CA3. The convergence of these internal and external representations in CA1 could lead to the emergence of episodic memory: a spatiotemporally ordered representation of experienced events. We indeed show that hippocampal run sequences can actually represent any type of spatiotemporal information. If an animal is trained for a given task, the hippocampus can readily adapt its integration of external inputs to represent the relevant information. For example, when a mouse is required to run for a fixed amount of time, as happens during the delay period of a spatial memory task, CA1 sequences will stretch to span and represent the entire duration of the task or, alternatively, be reused to represent the different locations the mouse will explore in a maze (2). This embedded sequential activity could serve as a template to temporally organize external inputs, such as sensory cues or emotional events, to form a memory (34). The template has to be flexible enough to represent different scales and different dimensions of the ongoing experience (33). Here we show that a recurrent network can represent both time and space and can scale without rewiring. Future experimental work should explore this possibility.

Materials and Methods

More details are provided in *SI Appendix*. Reported values are mean ± SD unless noted otherwise. All protocols were performed in accordance with the guidelines of the French National Ethics Committee for Sciences and Health report "Ethical Principles for Animal Experimentation," in agreement with European Community Directive 86/609/EEC. The experimental protocols were approved by the French National Ethics Committee under agreement 01413.03.

Spatiotemporal Tests. Correlations among sequence slopes in different spatiotemporal domains and mouse speeds were used to test for spatiotemporal representation. In the temporal test, sequence slopes were measured in the spatial domain; in the spatial test, they were measured in the temporal domain; and in the spatiotemporal test, sequence slopes were measured in a spatiotemporal domain (*SI Appendix*).

Data Sharing. Data samples can be downloaded from figshare (https://doi.org/10.6084/m9.figshare.5531770.v1). All data and codes used in analysis and for the model are available on GitHub, https://github.com/CarolineHaimerl27/duration_distance_coding.git.

ACKNOWLEDGMENTS. This project received funding from the European Research Council under FP7 and H2020 Program Grants 242842 and 646925; German Research Foundation Grant RE 3657/1-1; William Harvey International Translational Research Academy Co-funding of regional, national and international programmes from European Commission (COFUND) Grant PCOFUND-GA-2013-608765 (to S.R.); and Aix-Marseille Initiative d'Excellence (A*MIDEX) Grant ANR-11-IDEX-0001-02, funded by the Programme Investissements d'Avenir (to D.A.-G. and A.T.).

1. Tulving E (1983) *Elements of Episodic Memory* (Oxford Univ Press, New York).
2. Pastalkova E, Itskov V, Amarasingham A, Buzsáki G (2008) Internally generated cell assembly sequences in the rat hippocampus. *Science* 321:1322–1327.
3. MacDonald CJ, Lepage KQ, Eden UT, Eichenbaum H (2011) Hippocampal "time cells" bridge the gap in memory for discontiguous events. *Neuron* 71:737–749.
4. Kraus BJ, Robinson RJ, 2nd, White JA, Eichenbaum H, Hasselmo ME (2013) Hippocampal "time cells": Time versus path integration. *Neuron* 78:1090–1101.
5. Villette V, Malvache A, Tressard T, Dupuy N, Cossart R (2015) Internally recurring hippocampal sequences as a population template of spatiotemporal information. *Neuron* 88:357–366.
6. Salz DM, et al. (2016) Time cells in hippocampal area CA3. *J Neurosci* 36:7476–7484.
7. Middleton SJ, McHugh TJ (2016) Silencing CA3 disrupts temporal coding in the CA1 ensemble. *Nat Neurosci* 19:945–951.
8. Hafting T, Fyhn M, Molden S, Moser MB, Moser EI (2005) Microstructure of a spatial map in the entorhinal cortex. *Nature* 436:801–806.
9. Kraus BJ, et al. (2015) During running in place, grid cells integrate elapsed time and distance run. *Neuron* 88:578–589.
10. Howard MW, et al. (2014) A unified mathematical framework for coding time, space, and sequences in the hippocampal region. *J Neurosci* 34:4692–4707.
11. Tsodyks MV, Skaggs WE, Sejnowski TJ, McNaughton BL (1996) Population dynamics and theta rhythm phase precession of hippocampal place cell firing: A spiking neuron model. *Hippocampus* 6:271–280.
12. Navratilova Z, Giocomo LM, Fellous J-M, Hasselmo ME, McNaughton BL (2012) Phase precession and variable spatial scaling in a periodic attractor map model of medial entorhinal grid cells with realistic after-spike dynamics. *Hippocampus* 22:772–789.
13. Wang Y, Romani S, Lustig B, Leonardo A, Pastalkova E (2015) Theta sequences are essential for internally generated hippocampal firing fields. *Nat Neurosci* 18:282–288.
14. Murray JM, Escola GS (2017) Learning multiple variable-speed sequences in striatum via cortical tutoring. *eLife* 6:e26084.
15. Rajan K, Harvey CD, Tank DW (2016) Recurrent network models of sequence generation and memory. *Neuron* 90:128–142.
16. Compte A, Brunel N, Goldman-Rakic PS, Wang XJ (2000) Synaptic mechanisms and network dynamics underlying spatial working memory in a cortical network model. *Cereb Cortex* 10:910–923.
17. Le Duigou C, Simonnet J, Teleñczuk MT, Fricker D, Miles R (2014) Recurrent synapses and circuits in the CA3 region of the hippocampus: An associative network. *Front Cell Neurosci* 7:262.
18. Guzman SJ, Schlögl A, Frotscher M, Jonas P (2016) Synaptic mechanisms of pattern completion in the hippocampal CA3 network. *Science* 353:1117–1123.
19. Klausberger T, Somogyi P (2008) Neuronal diversity and temporal dynamics: The unity of hippocampal circuit operations. *Science* 321:53–57.
20. Buzsáki G (2002) Theta oscillations in the hippocampus. *Neuron* 33:325–340.
21. Dombeck DA, Harvey CD, Tian L, Looger LL, Tank DW (2010) Functional imaging of hippocampal place cells at cellular resolution during virtual navigation. *Nat Neurosci* 13:1433–1440.
22. Romani S, Tsodyks M (2015) Short-term plasticity-based network model of place cells dynamics. *Hippocampus* 25:94–105.
23. Debanne D, Inglebert Y, Russier M (2018) Plasticity of intrinsic neuronal excitability. *Curr Opin Neurobiol* 54:73–82.
24. Salin PA, Scanziani M, Malenka RC, Nicoll RA (1996) Distinct short-term plasticity at two excitatory synapses in the hippocampus. *Proc Natl Acad Sci USA* 93:13304–13309.
25. Miles R, Wong RK (1986) Excitatory synaptic interactions between CA3 neurones in the guinea-pig hippocampus. *J Physiol* 373:397–418.
26. Richard GR, et al. (2013) Speed modulation of hippocampal theta frequency correlates with spatial memory performance. *Hippocampus* 23:1269–1279.
27. Ziv Y, et al. (2013) Long-term dynamics of CA1 hippocampal place codes. *Nat Neurosci* 16:264–266.
28. Fuhrmann F, et al. (2015) Locomotion, theta oscillations, and the speed-correlated firing of hippocampal neurons are controlled by a medial septal glutamatergic circuit. *Neuron* 86:1253–1264.
29. Goaillard JM, Taylor AL, Pulver SR, Marder E (2010) Slow and persistent postinhibitory rebound acts as an intrinsic short-term memory mechanism. *J Neurosci* 30:4687–4692.
30. Colgin LL (2015) Theta-gamma coupling in the entorhinal-hippocampal system. *Curr Opin Neurobiol* 31:45–50.
31. Hulse BK, Lubenov EV, Siapas AG (2017) Brain state dependence of hippocampal subthreshold activity in awake mice. *Cell Rep* 18:136–147.
32. Sandler RA, Fetterhoff D, Hampson RE, Deadwyler SA, Marmarelis VZ (2017) Cannabinoids disrupt memory encoding by functionally isolating hippocampal CA1 from CA3. *PLoS Comput Biol* 13:e1005624.
33. Eichenbaum H (2017) On the integration of space, time, and memory. *Neuron* 95:1007–1018.
34. Buzsáki G, Tingley D (2018) Space and time: The hippocampus as a sequence generator. *Trends Cogn Sci* 22:853–869.